Journal of Minerals and Materials Characterization and Engineering, 2014, 2, 545-553
Published Online November 2014 in SciRes. http://www.scirp.org/journal/jmmce
http://dx.doi.org/10.4236/jmmce.2014.26056

Enhanced High-Temperature Cycling Stability of $LiMn_2O_4$ by Coating $LiNi_{0.5}Mn_{1.5}O_4$

Jing Yan[1], Wei Liu[2,3], Yuelei Wang[1], Xinxin Zhao[1], Yiming Mi[1], Haohan Liu[2,3*]

[1]College of Chemistry and Chemical Engineering, Shanghai University of Engineering Science, Shanghai, China
[2]Shanghai Nanotechnology Promotion Center, Shanghai, China
[3]Shanghai Institute of Microsystem and Information Technology, Chinese Academy of Sciences, Shanghai, China
Email: *biluo1873@163.com

Received 25 August 2014; revised 17 October 2014; accepted 28 October 2014

Academic Editor: Jiann-Yang (Jim) Hwang, Michigan Technological University, USA

Abstract

To enhance the electrochemical performances of $LiMn_2O_4$ at elevated temperature (55˚C), we proposed a sol-gel method to synthesize $LiNi_{0.5}Mn_{1.5}O_4$ modified $LiMn_2O_4$. The physical and electrochemical performances of pristine and $LiNi_{0.5}Mn_{1.5}O_4$-coated $LiMn_2O_4$ cathode materials were investigated by X-ray diffraction, scanning electron microscopy, transmission electron microscopy, X-ray photoelectron spectroscopy and electrochemical measurements, respectively. The results indicated that about 4 - 5 nm thick layer of $LiNi_{0.5}Mn_{1.5}O_4$ was formed on the surface of the $LiMn_2O_4$ powders. The modified $LiMn_2O_4$ exhibited excellent storage performance at 55˚C compared to the pristine one, which was attributed to the suppression of electrolyte decomposition and the reduction of Mn dissolution.

Keywords

$LiMn_2O_4$, Sol-Gel Method, Surface Coating, Electrochemical Performance

1. Introduction

With the advantages of abundant, nontoxic, and inexpensive, spinel lithium manganese oxide ($LiMn_2O_4$) is a promising candidate of the layered cathode materials such as $LiCoO_2$ [1] [2]. Especially, the good stability of $LiMn_2O_4$ may ensure its large-scale usage in the batteries for electric vehicle or energy storage [3]. However, $LiMn_2O_4$ shows obvious capacity fade when cycling at high temperature [4]-[6]. It was reported that the capacity fading mechanism at high temperature was related to the Jahn-Teller distortion and dissolution of Mn^{3+} ions

*Corresponding author.

How to cite this paper: Yan, J., Liu, W., Wang, Y.L., Zhao, X.X., Mi, Y.M. and Liu, H.H. (2014) Enhanced High-Temperature Cycling Stability of $LiMn_2O_4$ by Coating $LiNi_{0.5}Mn_{1.5}O_4$. *Journal of Minerals and Materials Characterization and Engineering*, **2**, 545-553. http://dx.doi.org/10.4236/jmmce.2014.26056

[7] [8]. Mn dissolution is induced by HF acid, which is generated by secondary chemical reactions from temperature-enhanced electrolyte decomposition.

In order to solve this problem, earlier studies have been focused on a chemical modification of $LiMn_2O_4$ by a partial substitution of Mn with some metal ions to obtain $LiM_xMn_{2-x}O_4$ (M = Co, Mg, Cr, Ni, Fe, Al, Ti and Zn) [9]-[12]. These results indicated that the substitution of Mn with metal ions significantly improved the cycle performance of $LiMn_2O_4$. However, the partial substitutions decrease the capacity of $LiMn_2O_4$. Another effective way is surface coating on $LiMn_2O_4$ by oxide with high thermal and structural stability. ZrO_2 [13], Al_2O_3 [14], SiO_2 [15] and MgO [16] have been used to coat $LiMn_2O_4$ by some chemical processes. However, the aforementioned oxides with non-spinel structure are hard to grow on the surface of $LiMn_2O_4$. With a similar structure to $LiMn_2O_4$, $LiNi_{0.5}Mn_{1.5}O_4$ can grow more easily on $LiMn_2O_4$ than other alien phase and form a more close-contacted protective covering layer, which may suppress the dissolution of Mn. Therefore, it is expected that the modified $LiMn_2O_4$ will show an excellent cycle performance at elevated temperature. In this study, we proposed an approach to synthesize $LiNi_{0.5}Mn_{1.5}O_4$ on the surface of spinel $LiMn_2O_4$. The effect of $LiNi_{0.5}Mn_{1.5}O_4$ layer on the morphology and electrochemical performances of $LiMn_2O_4$ cathode materials were examined in detail.

2. Experimental

$LiMn_2O_4$ powder was purchased from Heibei Strong-Power Li-ion Battery Tecnology Co. Ltd (D98, China). To coat $LiMn_2O_4$ with $LiNi_{0.5}Mn_{1.5}O_4$, $LiCH_3COO·2H_2O$ (0.558 g), Mn $(CH_3COO)_2·4H_2O$ (2.011 g) and Ni $(CH_3COO)_2·4H_2O$ (0.68 g) with a stoichiometric ratio (2:1:3) were dissolved in distilled water to form a clear solution. An aqueous solution of ethylene glycol and citric acid as a chelating agent was added to the mixtures. pH value at 6.5 - 7.0 was achieved by Ammonium hydroxide. Then the $LiMn_2O_4$ powders (50 g) were slowly added to the sol and vigorously stirred at 85˚C for 8 h. As the evaporation of water proceeding, the sol was turned into a viscous transparent gel. After drying and sieving, the powder was sintering in air at 400˚C for 10 h and 750˚C for 3 h to obtain $LiNi_{0.5}Mn_{1.5}O_4$-coated $LiMn_2O_4$. For a comparison, pristine $LiMn_2O_4$ was also heat-treated in the same condition.

2.1. Structure and Morphology Characterization

X-ray diffraction patterns were recorded on a DX-2700 diffractometer (Siemens D-5000, Mac Science MXP 18) equipped with Cu Kα radiation of λ = 0.154145 nm. The diffraction patterns were recorded between scattering angles of 15˚ and 80˚ at a step of 4˚/min. The morphology was studied by a scanning electron microscopy (S4700, Hitachi) and transmission electron microscope (JEOL-1200EX). X-ray photoelectron spectroscopy (Kratos AXIS Ultra DLD) was employed to probe the surface for Mn Valence states. Inductively coupled plasma atomic emission spectrometry analysis was conducted on IRIS Intrepid Π XSP inductively coupled plasma emission spectrometer (THERMO).

2.2. Electrochemical and Thermal Characteristics

To obtain working electrodes, 85 wt% active materials, 9 wt% acetylene black and 6 wt% polyvinylidene fluoride were homogeneously mixed in N-methyl-pyrroline. Then the resluting slurry was spread on an aluminum foil and thoroughly dried. The electrodes were punched in the form of 14 mm diameter disks, and the typical active material mass loading was about 6 mg/cm^2. The electrolyte was 1 M $LiPF_6$ dissolved in a mixture of ethylene carbonate and dimethylene carbonate with the volume ratio of 1:1. The assembly process was conducted in an argon-filled glove-box with the content of H_2O and O_2 less than 1 ppm.

Before electrochemical tests, the batteries were aged for 24 h to ensure good soakage. The cells were charged and discharged on a battery tester (CT-3008W, NEWARE) between 3.3 and 4.35 V at the rate of 2C at elevated temperatures (55˚C ± 2˚C). Cyclic voltammetry (CV) and electrochemical impedance spectroscopy (EIS) investigations were performed on an electrochemical workstation (PGSTAT302N, Autolab) at 25˚C ± 2˚C. The CV curves were recorded between 3.3 and 4.35 V at a scan rate of 0.1 $mV·s^{-1}$. The EIS measurements were performed over a frequency range from 10 kHz to 0.1 Hz.

3. Results and Discussion

Figure 1 shows the XRD patterns of pristine and $LiNi_{0.5}Mn_{1.5}O_4$-coated $LiMn_2O_4$. The peaks of both samples could be indexed to a cubic spinel structure with the space group Fd3m. There is no substantial difference between XRD patterns for pristine and modified $LiMn_2O_4$. The crystal lattice parameters were calculated by using the software of Jade, are 8.245 and 8.243 Å for the pristine and $LiNi_{0.5}Mn_{1.5}O_4$-coated $LiMn_2O_4$, indicating that the bulk structure of $LiMn_2O_4$ unchange after surface modification. The characteristic peaks corresponding to $LiNi_{0.5}Mn_{1.5}O_4$ are not observed because of the low content (about 2.0 wt%).

Scanning electron microscopy reveals that the pristine and modified samples present a uniform particle distribution, ranging from 2 to 7 μm. The pristine spinel crystals are smooth with well-defined facets, as observed in **Figure 2(a)** and **Figure 2(c)**. It can be seen that the morphology and particle diameter of the $LiNi_{0.5}Mn_{1.5}O_4$-

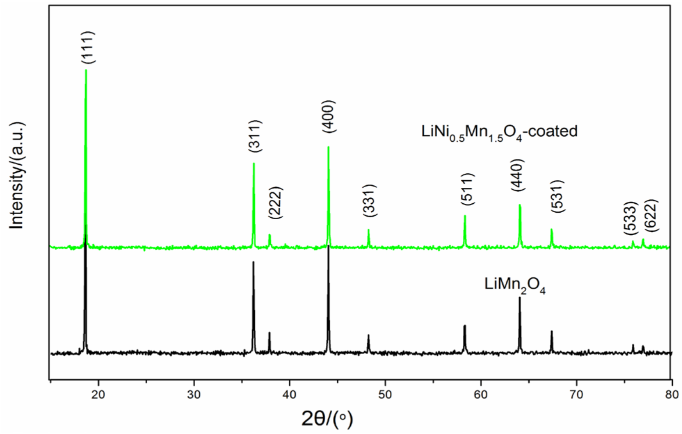

Figure 1. X-ray diffraction patterns of pristine and modified $LiMn_2O_4$.

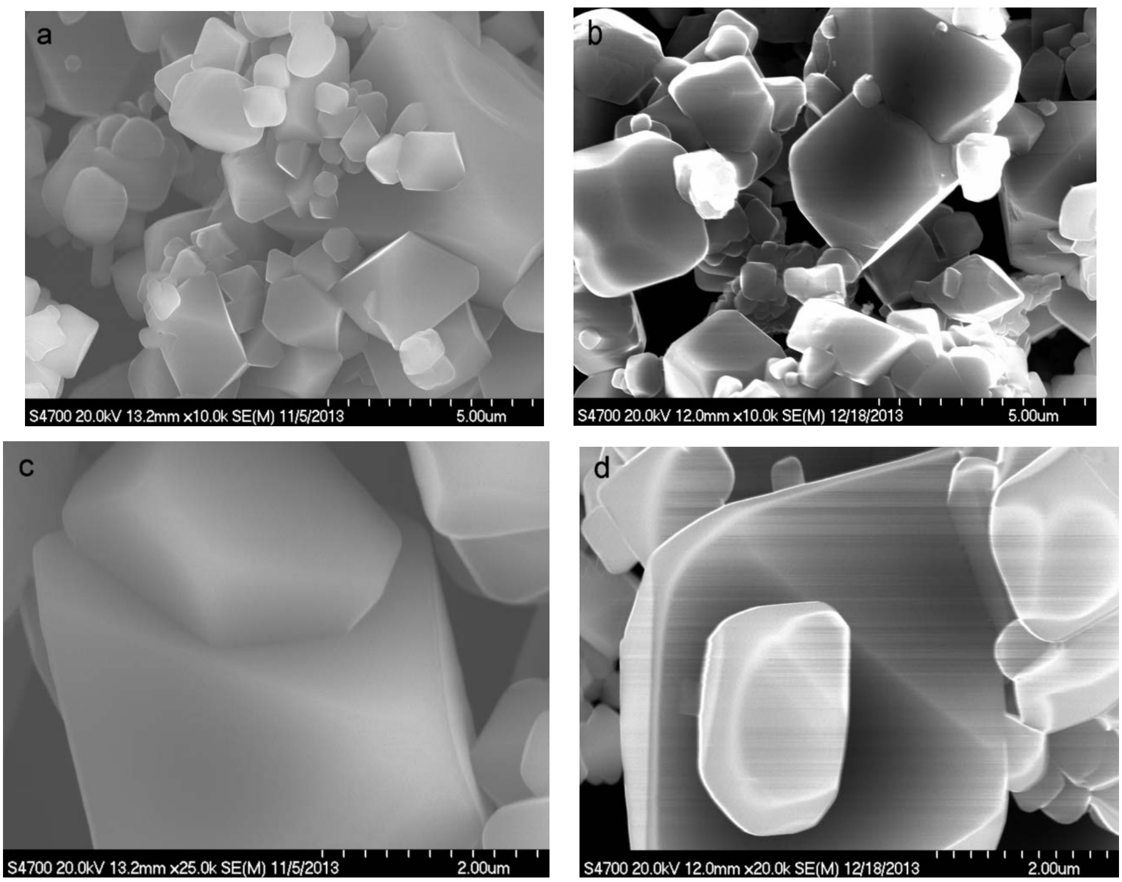

Figure 2. SEM figures of (a), (c) pristine and (b), (d) $LiNi_{0.5}Mn_{1.5}O_4$-coated $LiMn_2O_4$.

coated $LiMn_2O_4$ powders in **Figure 2(b)** and **Figure 2(d)**, are similar to the pristine sample. No $LiNi_{0.5}Mn_{1.5}O_4$ agglomerations and obscured facets of spinel $LiMn_2O_4$ are observed.

The element composition is determined by EDS analysis. The element mapping of Ni and Mn is displayed in **Figure 3**. The dense accumulation of Mn spots is attributed to the host material of $LiMn_2O_4$ and there is no significant agglomeration of Ni. This indicates that $LiNi_{0.5}Mn_{1.5}O_4$ is homogeneously dispersed on the surface of the $LiMn_2O_4$ particles.

TEM micrographs are displayed in **Figure 4**. Compared to the pristine sample (**Figure 4(a)**), about 4 - 5 nm

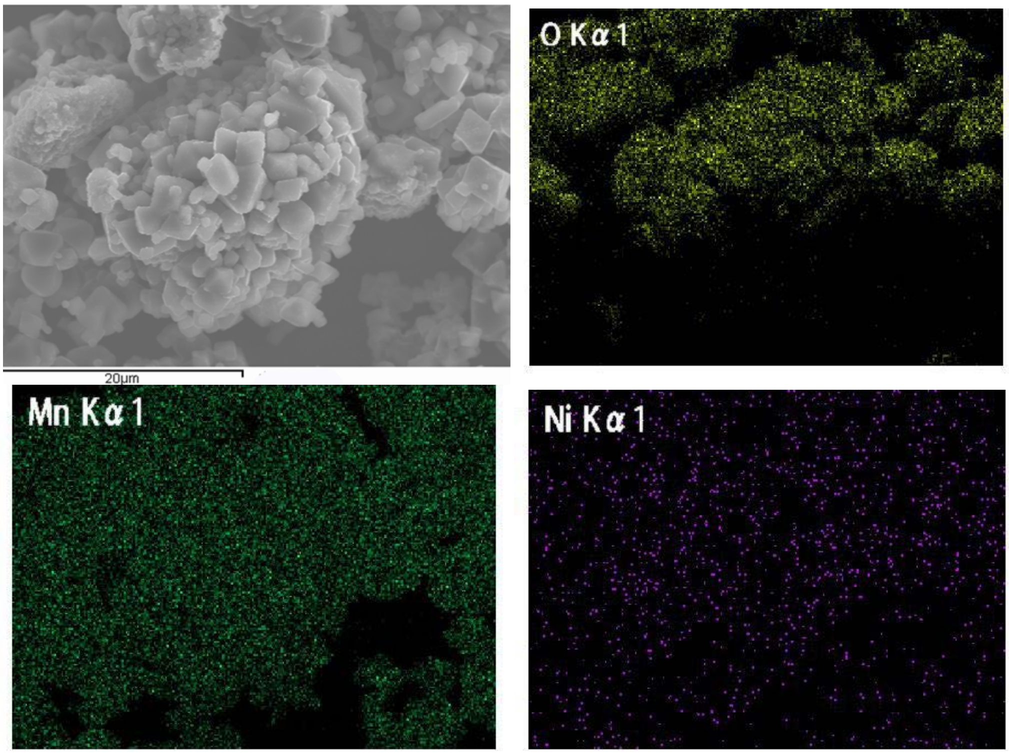

Figure 3. EDS mappings of O, Mn and Ni elements of modified $LiMn_2O_4$.

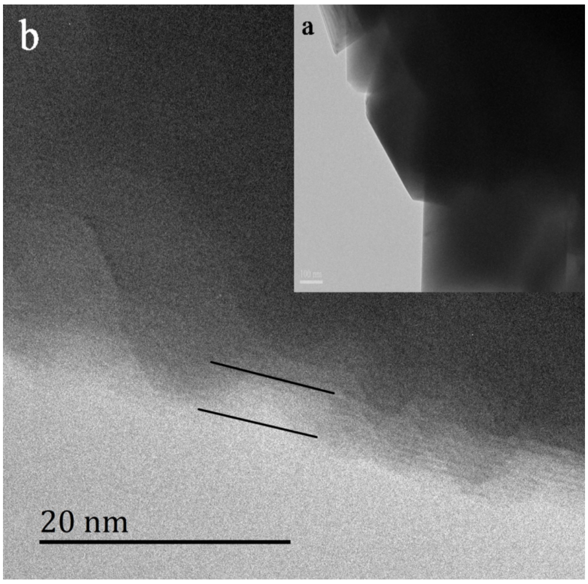

Figure 4. TEM figure of pristine (a) and $LiNi_{0.5}Mn_{1.5}O_4$-coated $LiMn_2O_4$ (b).

thick layer of $LiNi_{0.5}Mn_{1.5}O_4$ is uniformly formed on the surface of the $LiMn_2O_4$ (**Figure 4(b)**). The coating layer is clearly distinguishable from the crystalline $LiMn_2O_4$. The TEM analysis demonstrates that the sol-gel method is an effective way to coat the $LiNi_{0.5}Mn_{1.5}O_4$ layer on the surface of $LiMn_2O_4$.

The oxidation state of manganese ions at the surface was determined from XPS data by the curve fitting of Mn 2p spectral peaks. The experimental peak shape for Mn $2p_{3/2}$ was modeled by employing multiple-splitting patterns derived for Mn^{3+} and Mn^{4+} at binding energies of 641.6, and 642.8 eV from the standard compounds Mn_2O_3 and MnO_2. **Figure 5** shows the fit of the models to the experimental spectra for pristine $LiMn_2O_4$ and $LiNi_{0.5}Mn_{1.5}O_4$-coated $LiMn_2O_4$ respectively. The surface of the pristine $LiMn_2O_4$ sample consists of almost equal amounts of Mn^{4+} and Mn^{3+}. By contrast, $LiNi_{0.5}Mn_{1.5}O_4$-coated $LiMn_2O_4$ exhibited a Mn^{4+}:Mn^{3+} ratio of 59.4:40.6. The difference of Mn^{4+}:Mn^{3+} ratio on the surface is due to the formation of $LiNi_{0.5}Mn_{1.5}O_4$, because it has higher valence state of manganese ions. This result is good agreement with the observation of HR-TEM.

As shown in **Figure 6**, the galvanostatic charge-discharge curves under a current rate of 2C were conducted at elevated temperatures (55˚C). It shows two discharge plateaus, which should be attributed to orderly intercalating of lithium ions in the tetrahedral (8a) sites at 4.1 V and disorderly intercalating lithium ions at 3.9 V which substantially maintains the intercalation feature of $LiMn_2O_4$ substrate [17], indicating $LiNi_{0.5}Mn_{1.5}O_4$ surface layer rather than Ni-doped $LiMn_2O_4$ because $LiMn_2O_4$ with Ni-doped spinel surface showed two ambiguously resolved discharging plateaus. $LiNi_{0.5}Mn_{1.5}O_4$-coated $LiMn_2O_4$ shows a lower discharge capacity (104.2 mAh/g) compares to the pristine sample (106.3 mAh/g). The reason of low initial discharge capacity is that $LiNi_{0.5}Mn_{1.5}O_4$ shows no capacity at this voltage range due to its high discharge voltage over 4.35V [18].

Figure 7 shows the cycling performance of electrodes with and without $LiNi_{0.5}Mn_{1.5}O_4$ coating. After 100 cycles, the discharge capacity of the pristine $LiMn_2O_4$ drops from 106.3 to 89.2 mAh/g. In contrast, the discharge capacity of modified sample changes from 104.2 to 98 mAh/g. The capacity retention increases from 84.0% to 94.4% after $LiNi_{0.5}Mn_{1.5}O_4$ coating.

To further verify the effects of surface coating on manganese ions dissolution, the quality of the manganese element was directly determined by using ICP-AES. Li metal anode was washed by dilute hydrochloric acid after 100th cycle at 55˚C ± 2˚C. It can be seen in **Table 1**, the dissolved quality of Mn^{2+} ions of the pristine and $LiNi_{0.5}Mn_{1.5}O_4$-coated $LiMn_2O_4$ electrode was 20.54 and 12.17 μg/cm², respectively. It can be concluded that after coating by $LiNi_{0.5}Mn_{1.5}O_4$ layer, the dissolution of the manganese ions was significantly reduced. Therefore, $LiNi_{0.5}Mn_{1.5}O_4$-coated $LiMn_2O_4$ electrode had better cycle stability at elevated temperature.

Figure 8 shows the CV profiles of pristine and $LiNi_{0.5}Mn_{1.5}O_4$-coated $LiMn_2O_4$ electrodes in the 10th and 100th cycles at the scan rate of 0.1 $mV \cdot s^{-1}$. The CV peaks of $LiNi_{0.5}Mn_{1.5}O_4$-coated sample show two symmetrical couples of redox peaks at around 3.98 and 4.1 V respectively (**Figure 8(b)**), indicating that electrochemical insertion and extraction reactions of Li^+ ions are two step processes. It is in agreement with the two plateaus in **Figure 6** and demonstrates that $LiNi_{0.5}Mn_{1.5}O_4$ coating does not change the electrochemical reaction mechanism of $LiMn_2O_4$. After 10 cycles, two narrow and separate redox peaks appear around at 3.96 and 4.11 V, as shown in **Figure 8(a)**. However, after 100th cycles, due to the dissolution of Mn^{3+} ions into the electrolyte

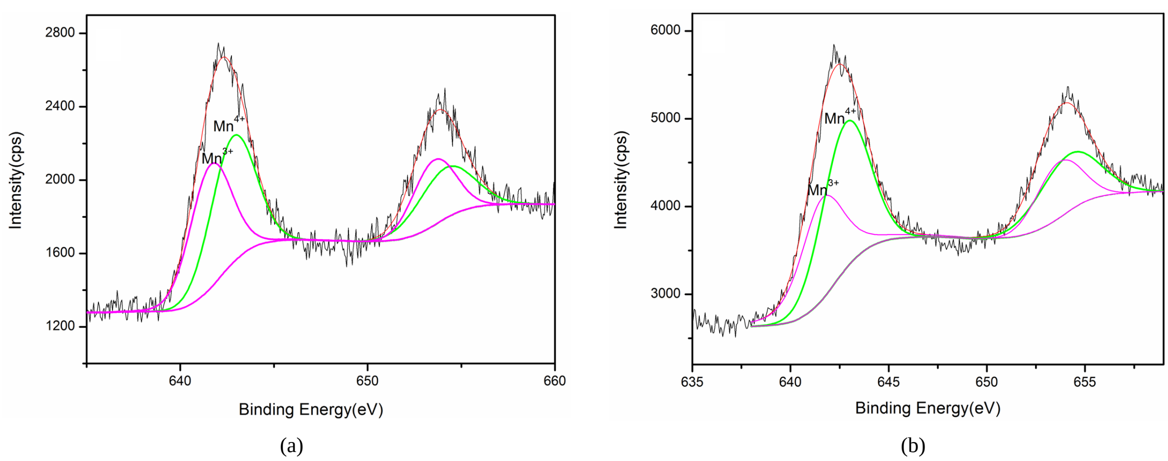

(a) (b)

Figure 5. XPS spectra of the pristine (a) and $LiNi_{0.5}Mn_{1.5}O_4$-coated $LiMn_2O_4$ (b).

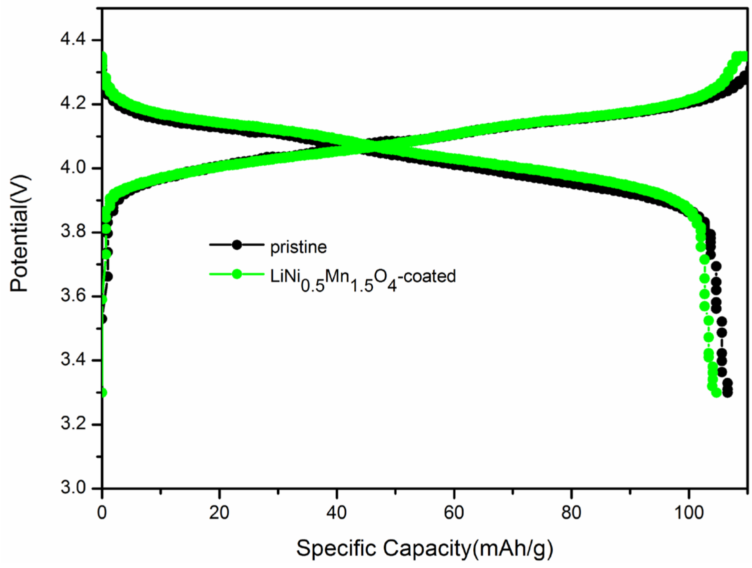

Figure 6. The first Charge-discharge curves of $LiNi_{0.5}Mn_{1.5}O_4$-coated $LiMn_2O_4$ at elevated temperature (under 2C rate, 55˚C ± 2˚C).

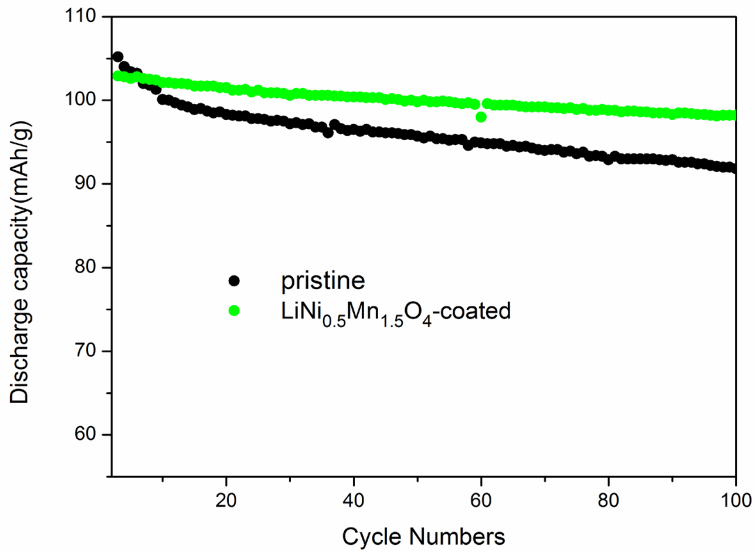

Figure 7. Cycling behaviours of $LiMn_2O_4$ and $LiNi_{0.5}Mn_{1.5}O_4$-coated $LiMn_2O_4$ cycled (under 2C rate, 55˚C ± 2˚C).

Table 1. The amount of Mn^{2+} deposited on Li anode after 100 cycles at 55˚C ± 2˚C.

Samples	The quality of Mn on Li anode (μg/cm^2)
Pristine $LiMn_2O_4$	20.54
$LiNi_{0.5}Mn_{1.5}O_4$-coated $LiMn_2O_4$	12.17

(Jahn-Teller distortion), both anodic and cathodic peaks become much broader and lower in peaks current. In contrast, the oxidation and reduction peaks relate to $LiNi_{0.5}Mn_{1.5}O_4$-coated $LiMn_2O_4$ are much steadier after 100 cycles (**Figure 8(b)**), which indicated that modified $LiMn_2O_4$ has better reversibility and stability than the pristine $LiMn_2O_4$.

Electrochemical impedance spectra (EIS) and equivalent circuits are shown in **Figure 9**. The measurements were carried out with fully charged state (4.35 V). An intercept in the high frequency region of the Z_{rel} axis indicates the ohmic resistance (Rs), the combined resistance of the electrolyte and the contacts of the cell [19]. The semicircle in high-middle frequency region corresponds to the charge transfer (Rct) process on the electrode interface, revealing the lithium transfer rate parameters and the capacitance of the SEI (solid eleteolyte interface) [20]. The inclined line in the lower frequency region represents the Warburg impedance (Zw), which is corresponded to the diffusion of Li^+ in $LiMn_2O_4$ particles [21]. The plots are fitted and listed in **Table 2**. As shown in

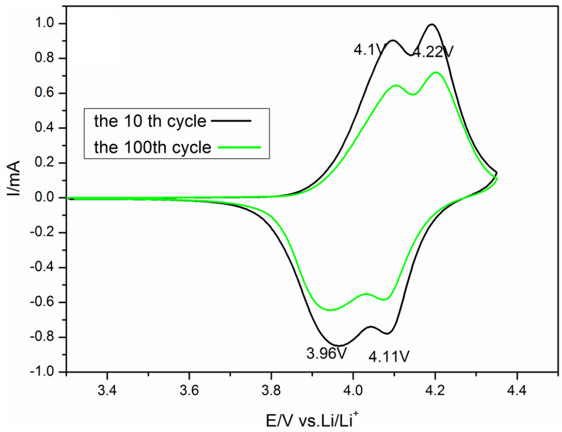

(a) (b)

Figure 8. Typical CV curves of 10th and 100th cycles of pristine (a), and $iNi_{0.5}Mn_{1.5}O_4$-coated $LiMn_2O_4$ (b).

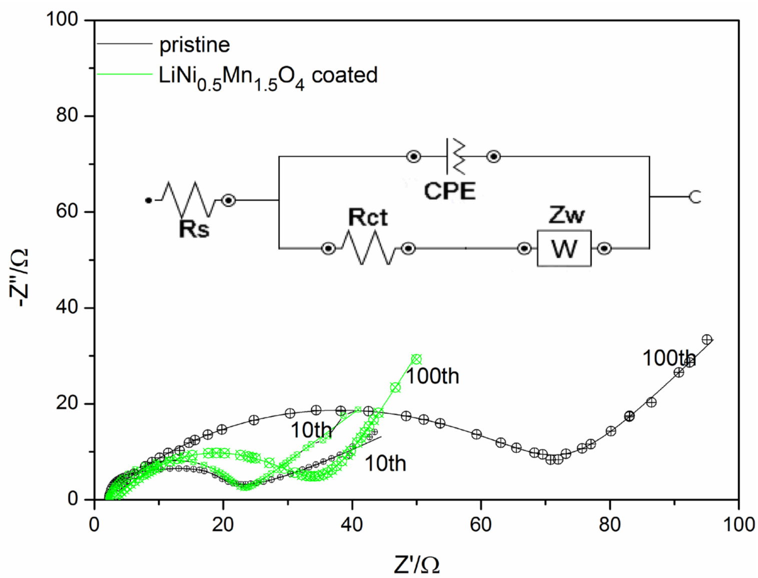

Figure 9. EIS of pristine and $LiNi_{0.5}Mn_{1.5}O_4$-coated $LiMn_2O_4$ at the end of 10th and 100th cycle.

Table 2. The AC impedance fitting data for pristine $LiMn_2O_4$ and $LiNi_{0.5}Mn_{1.5}O_4$-coated $LiMn_2O_4$.

Samples	R_s/Ω	R_{ct}/Ω
Pristine $LiMn_2O_4$ at 10th fully charge state	2.02	26.82
$LiNi_{0.5}Mn_{1.5}O_4$-coated $LiMn_2O_4$ at 10th fully charged state	2.20	24.4
Pristine $LiMn_2O_4$ at 100th fully charge state	3.55	73.8
$LiNi_{0.5}Mn_{1.5}O_4$-coated $LiMn_2O_4$ at 100th fully charged state	2.85	34.8

the table, after 10 cycles, the Rs for $LiNi_{0.5}Mn_{1.5}O_4$-coated $LiMn_2O_4$ is slightly larger than the pristine sample, because that the coating layer may slightly increase the electrolyte and contact resistance. The charge transfer resistance of both samples is approximately the similar (26.82 and 24.4 $\Omega\cdot cm^2$). After 100 cycles, the change in R_s is negligible. However, the R_{ct} value of the $LiNi_{0.5}Mn_{1.5}O_4$-coated electrode (34.8 $\Omega\cdot cm^2$) is two times smaller than that the value pristine electrode (73.8 $\Omega\cdot cm^2$). It attributes to the restraint of structural instability caused by the subsequent Mn dissolution and vacancies formation. This result is also in accordance with the enhanced cycling performance of $LiNi_{0.5}Mn_{1.5}O_4$-coated electrodes.

4. Conclusion

In summary, the surface of $LiMn_2O_4$ sample was modified by $LiNi_{0.5}Mn_{1.5}O_4$ using a sol-gel method. TEM and XPS results confirm the existence of $LiNi_{0.5}Mn_{1.5}O_4$ layer. A uniform and dense layer about 4 - 5 nm was coating on the surface of pristine $LiMn_2O_4$. The $LiNi_{0.5}Mn_{1.5}O_4$-coated $LiMn_2O_4$ sample exhibits much better cycling stability at elevated temperature (55˚C) compared with the pristine sample. The CV tests indicated that the $LiNi_{0.5}Mn_{1.5}O_4$-coated $LiMn_2O_4$ electrode has better reversibility and stability. Meanwhile, the charge transfer resistance of the $LiNi_{0.5}Mn_{1.5}O_4$-coated $LiMn_2O_4$ was much less than that of pristine sample after 100 cycles, which is ascribed to the better structural stability and restraint of Mn dissolution. These results demonstrated that this is an effective way to improve the high-temperature cyclic performance of spinel $LiMn_2O_4$.

Acknowledgements

This work was supported by National Science Foundation of China (No. 50672026). This work was also supported by Shanghai Nano Technology Promotion (No. 12ZR1448800).

References

[1] Pitchai, R., Thavasi, V., Mhaisalkar, S.G. and Ramakrishna, S. (2011) Nanostructured Cathode Materials: A Key for Better Performance in Li-Ion Batteries. *Journal of Materials Chemistry*, **21**, 11040-11051. http://dx.doi.org/10.1039/c1jm10857c

[2] Zhao, S., Bai, Y., Ding, L.H., Wang, B. and Zhang, W.F. (2013) Enhanced Cycling Stability and Thermal Stability of YPO_4-Coated $LiMn_2O_4$ Cathode Materials for Lithium Ion Batteries. *Solid State Ionics*, **247**, 22-29. http://dx.doi.org/10.1016/j.ssi.2013.05.022

[3] Kim, W.-K., Han, D.-W., Ryu, W.-H., Lim, S.-J. and Kwon, H.-S. (2012) Al_2O_3 Coating on $LiMn_2O_4$ by Electrostatic Attraction Forces and Its Effects on the High Temperature Cyclic Performance. *Electrochimica Acta*, **71**, 17-21. http://dx.doi.org/10.1016/j.electacta.2012.03.090

[4] Aoshima, T., Okahara, K., Kiyohara, C. and Shizuka, K. (2001) Mechanisms of Manganese Spinels Dissolution and Capacity Fade at High Temperature. *Journal of Power Sources*, **97-98**, 377-380. http://dx.doi.org/10.1016/S0378-7753(01)00551-1

[5] Baba, M., Kumagai, N., Fujita, H., Ohta, K., Nishidate, K., Komaba, S., Kaplan, B., Groult, H. and Devilliers, D. (2003) Multi-Layered Li-Ion Rechargeable Batteries for a High-Voltage and High-Current Solid-State Power Source. *Journal of Power Sources*, **119**, 914-917. http://dx.doi.org/10.1016/S0378-7753(03)00223-4

[6] Kim, D., Park, S., Chae, O.B., Ryu, J.H., Kim, Y.U., Yin, R.Z. and Oh, S.M. (2012) Re-Deposition of Manganese Species on Spinel $LiMn_2O_4$ Electrode after Mn Dissolution. *Journal of the Electrochemical Society*, **159**, A193-A197. http://dx.doi.org/10.1149/2.003203jes

[7] Gummow, R.J., Dekock, A. and Thackeray, M.M. (1994) Improved Capacity Retention in Rechargeable 4 V Lithium/Lithium-Manganese Oxide (Spinel) Cells. *Solid State Ionics*, **69**, 59-67. http://dx.doi.org/10.1016/0167-2738(94)90450-2

[8] Jang, D.H., Shin, Y.J. and Oh, S.M. (1996) Dissolution of Spinel Oxides and Capacity Losses in 4V $Li/Li_xMn_2O_4$ Coils. *Journal of the Electrochemical Society*, **143**, 2204-2211. http://dx.doi.org/10.1149/1.1836981

[9] Wu, X.L. and Kim, S.B. (2002) Improvement of Electrochemical Properties of $LiNi_{0.5}Mn_{1.5}O_4$ Spinel. *Journal of Power Sources*, **109**, 53-57. http://dx.doi.org/10.1016/S0378-7753(02)00034-4

[10] Tarascon, J.M., Wang, E., Shokoohi, F.K., McKinnon, W.R. and Colson, S. (1991) The Spinel Phase of $LiMn_2O_4$ as a Cathode in Secondary Lithium Cells. *Journal of the Electrochemical Society*, **138**, 2859-2864. http://dx.doi.org/10.1149/1.2085330

[11] Hernan, L., Morales, J., Sanchez, L. and Santos, J. (1999) Use of Li-M-Mn-O [M = Co, Cr, Ti] Spinels Prepared by a Sol-Gel Method as Cathodes in High-Voltage Lithium Batteries. *Solid State Ionics*, **118**, 179-185.

http://dx.doi.org/10.1016/S0167-2738(98)00449-4

[12] Thackeray, M.M., Johnson, C.S., Kim, J.S., Lauzze, K.C., Vaughey, J.T., Dietz, N., Abraham, D., Hackney, S.A., Zeltner, W. and Anderson, M.A. (2003) ZrO_2- and Li_2ZrO_3-Stabilized Spinel and Layered Electrodes for Lithium Batteries. *Electrochemistry Communications*, **5**, 752-758. http://dx.doi.org/10.1016/S1388-2481(03)00179-6

[13] Cho, J., Kim, Y.J., Kim, T.J. and Park, B. (2001) Enhanced Structural Stability of O-$LiMnO_2$ by Sol-Gel Coating of Al_2O_3. *Chemistry of Materials*, **13**, 18-20.http://dx.doi.org/10.1021/cm000759+

[14] Zheng, Z.H., Tang, Z.L., Zhang, Z.T., Shen, W.C. and Lin, Y.H. (2002) Surface Modification of $Li_{1.03}Mn_{1.97}O_4$ Spinels for Improved Capacity Retention. *Solid State Ionics*, **148**, 317-321. http://dx.doi.org/10.1016/S0167-2738(02)00068-1

[15] Gnanaraj, J.S., Pol, V.G., Gedanken, A. and Aurbach, D. (2003) Improving the High-Temperature Performance of $LiMn_2O_4$ Spinel Electrodes by Coating the Active Mass with MgO via a Sonochemical Method. *Electrochemistry Communications*, **5**, 940-945. http://dx.doi.org/10.1016/j.elecom.2003.08.012

[16] Wu, F., Wang, M., Su, Y.F., Chen, S. and Xu, B. (2009) Effect of TiO_2-Coating on the Electrochemical Performances of $LiCo_{1/3}Ni_{1/3}Mn_{1/3}O_2$. *Journal of Power Sources*, **191**, 628-632. http://dx.doi.org/10.1016/j.jpowsour.2009.02.063

[17] He, X.M., Li, J.J., Cai, Y., Wang, Y.W., Ying, J.R., Jiang, C.Y. and Wan, C.R. (2005) Preparation of Co-Doped Spherical Spinel $LiMn_2O_4$ Cathode Materials for Li-Ion Batteries. *Journal of Power Sources*, **150**, 216-222. http://dx.doi.org/10.1016/j.jpowsour.2005.02.029

[18] Myung, S.T., Izumi, K., Komaba, S., Sun, Y.K., Yashiro, H. and Kumagai, N. (2005) Role of Alumina Coating on Li-Ni-Co-Mn-O Particles as Positive Electrode Material for Lithium-Ion Batteries. *Chemistry of Materials*, **17**, 3695-3704. http://dx.doi.org/10.1021/cm050566s

[19] Jang, S.B., Kang, S.H., Amine, K., Bae, Y.C. and Sun, Y.K. (2005) Synthesis and Improved Electrochemical Performance of Al $(OH)_3$-Coated $Li[Ni_{1/3}Mn_{1/3}Co_{1/3}]O_2$ Cathode Materials at Elevated Temperature. *Electrochimica Acta*, **50**, 4168-4173. http://dx.doi.org/10.1016/j.electacta.2005.01.037

[20] Levi, M.D., Gamolsky, K., Aurbach, D., Heider, U. and Oesten, R. (2000) On Electrochemical Impedance Measurements of $Li_xCo_{0.2}Ni_{0.8}O_2$ and Li_xNiO_2 Intercalation Electrodes. *Electrochimica Acta*, **45**, 1781-1789. http://dx.doi.org/10.1016/S0013-4686(99)00402-8

[21] Fey, G.T.K., Lu, C.Z. and Kumar, T.P. (2003) Preparation and Electrochemical Properties of High-Voltage Cathode Materials, $LiM_yNi_{0.5-y}Mn_{1.5}O_4$ (M = Fe, Cu, Al, Mg; y = 0.0 - 0.4). *Journal of Power Sources*, **115**, 332-345. http://dx.doi.org/10.1016/S0378-7753(03)00010-7